Towards a realtime earthquake source determination and tsunami early warning in Northern California

Aurélie Guilhem and Douglas S. Dreger - Berkeley Seismological Laboratory

Abstract

The Mendocino Triple Junction (MTJ) is the most seismically active region of Northern California and it presents a variety of anomalous seismic events including repeating earthquakes, slow/low-stress-drop earthquakes, and non-volcanic tremors, in addition to typical inter- and intra-plate seismic activity. The seismicity extends to 40 km depth and includes potential large earthquakes (M7+) on the Mendocino transform fault, intra-plate events occurring in the offshore Gorda/Juan-de-Fuca plates and potential damaging thrust earthquakes along the adjacent segment of the Cascadia subduction zone (Oppenheimer et al., 1993). The current realtime earthquake monitoring in Northern California is a joint effort between the USGS Menlo Park and the Berkeley Seismological Laboratory at UC Berkeley. It is a cascade-type process in which the successive information of an earthquake is based on the previous parameter(s) obtained (i.e. location, origin time and magnitudes). For offshore earthquakes that are occurring outside of the seismic network like it is the case in the Mendocino region as well as along island arcs such a procedure can generate errors in the detection and location of the events and result in the incorrect determination of their characteristics (i.e. location, timing, moment magnitude and mechanism).

In the goal of more efficiently monitoring the offshore region, particularly for slow/low-stress-drop and large possibly tsunamigenic earthquakes, we develop an automatic scanning of continuous long-period (> 10 sec) broadband seismic records following the method proposed by Kawakatsu (1998) and implemented by Tsuruoka et al. (2009). In addition, we are proposing an improved algorithm for great events occurring on the CSZ, that if done in realtime with a continuous scanning algorithm, will provide information that could be eventually utilized for near-source tsunami early warning.

A continuous moment tensor algorithm

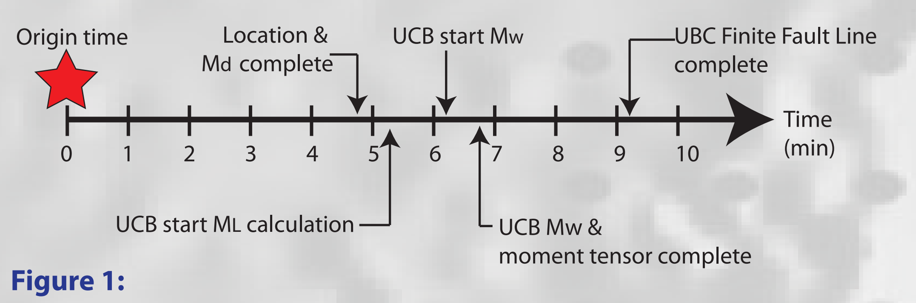

Figure 1:
Timeline of the current realtime procedure in Northern California

The current realtime procedure for earthquakes in Northern California is a cascade-type procedure (Figure 1). As soon as an earthquake is detected estimations of the magnitude and location are computed and from those results a moment analysis is eventually performed if the ML >=3.5.

Such a procedure fails if the preliminary location is incorrect, as well as the magnitude, and it potentially triggers a wrong seismic moment study. This is particularly problematic for the monitoring of slow/low-stress-drop earthquakes (Figure 2) observed in the vicinity of the triple junction as well as for large thrust earthquakes that could potentially be tsunamigenic.

We are implementing a continuous seismic scanning algorithm following the method proposed by Kawakatsu in 1998 and in used in Japan (Tsuruoka et al., 2009) that calculates moment tensors every 2 sec for each point of a grid (Figure 2) on filtered seismic data.

Characteristics of the analysis:

Grid search between:
- latitude: 40.0 and 43.0
- longitude: -123.0 and -128.0 (0.2 degree interval)
- depth: 5 and 38 km (3 km interval)
- a total of nearly 5,000 virtual sources

A catalog of Green's functions using a 1D velocity model

Four broadband Berkeley stations (HUMO, ORV, WDC, and YBH)

Two parallel-running systems:
- Inversion of 380 points of data filtered between 20-50 sec period for M<=7 earthquakes (Table 1)
- Inversion of 480 points of data filtered between 100-200 sec period for M>7 earthquakes

The earthquakes are detected once the variance reduction (VR) is above a fixed threshold (i.e. 65 % in Japan)

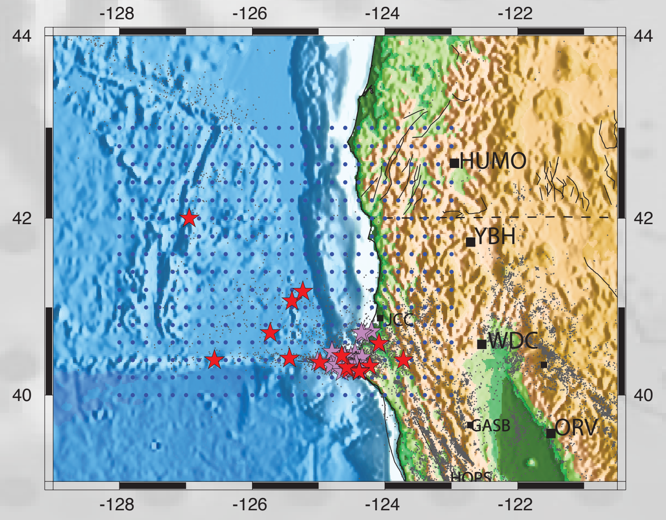

Figure 2: Map of the study region.
The seismicity from the ANSS catalog between 2000 and 2009 is shown by the gray dots and the broadband seismic stations of the Berkeley network by the black squares. The red and purple stars locate the slow/low-stress-drop and repeating earthquakes, respectively. The grid used in the study is shown by the small blue circles.

Event	Catalog	Inversion	Magnitude difference	Horizontal difference (km)	Vertical difference (km)	Time difference (sec)	VR (%)
2008 M4.2			0	22.5	8	4	79.9
2006 M5.0			0.1	23.5	2	6	80
2008 M5.4			0.1	9.1	2	4	69.7
2005 M6.7			0	4.7	17	2	78.4
2005 M7.0			0	9.8	17	14	76.2

Table 1: Preliminary results for earthquakes with magnitudes ranging from 4 to 7 in the Mendocino region.
The black mechanism is from the Berkeley Moment Tensor Catalog and is directly compared with the red mechanism that shows our best solution (largest VR) obtained between 20 and 50 sec period. Differences in magnitude and location are between the catalog solution and our solution.

Detecting a M8+ earthquake

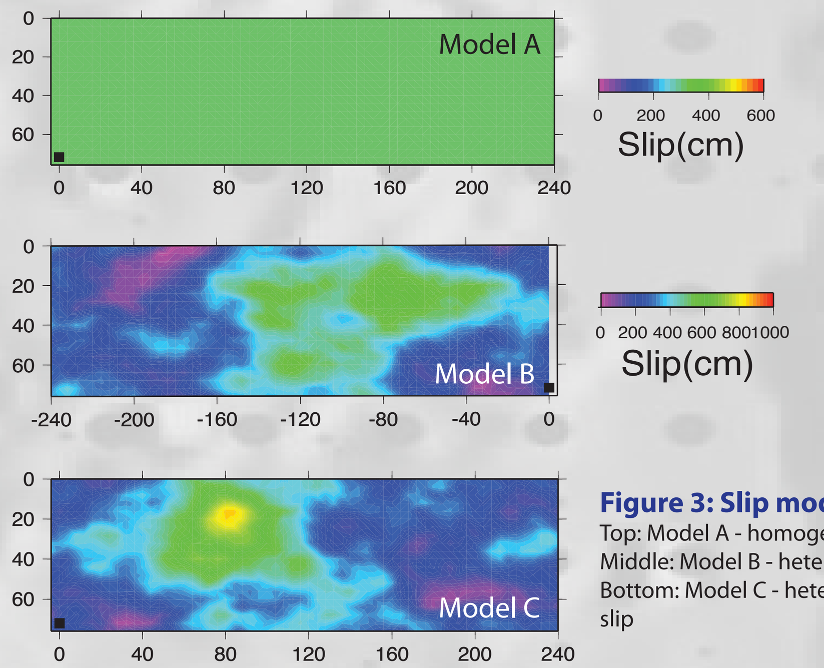

There is no available seismic data of a magnitude 8+ earthquake in our study region.

We performed a series of synthetic tests for large earthquakes (M>8) defined with uniform and variable slip models (Figure 3) along the Cascadia subduction zone.

Figure 3: Slip models of synthetic M8.2 earthquake.
Top: Model A - homogeneous slip.
Middle: Model B - heterogeneous slip.
Bottom: Model C - heterogeneous slip with a more concentrated slip

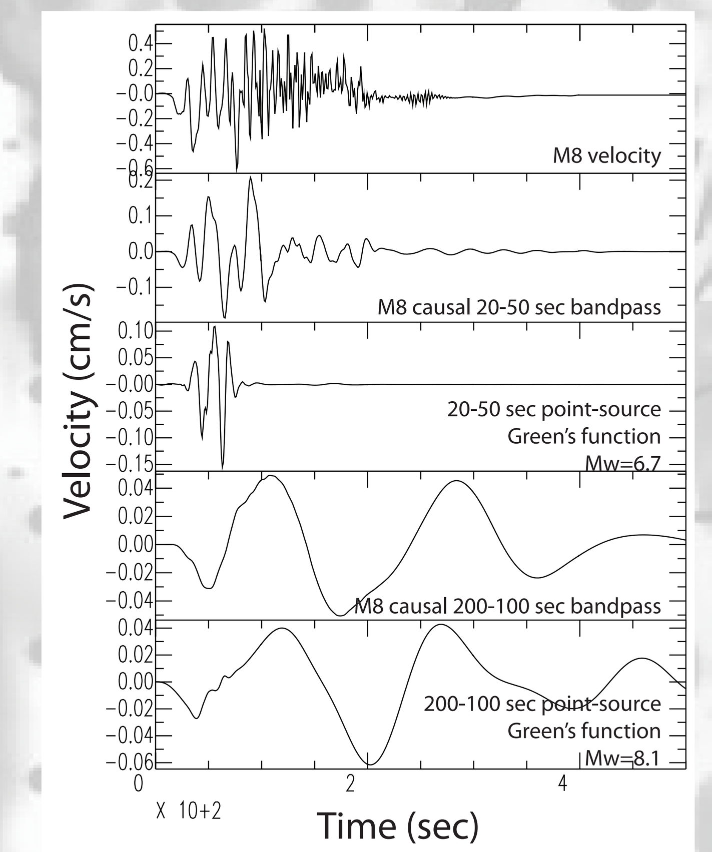

Figure 4: Comparison of the frequency bands (0.02-0.05 and 0.005-0.01 Hz) and corresponding Green's functions for a Magnitude 8 earthquake along the Cascadia subduction zone.

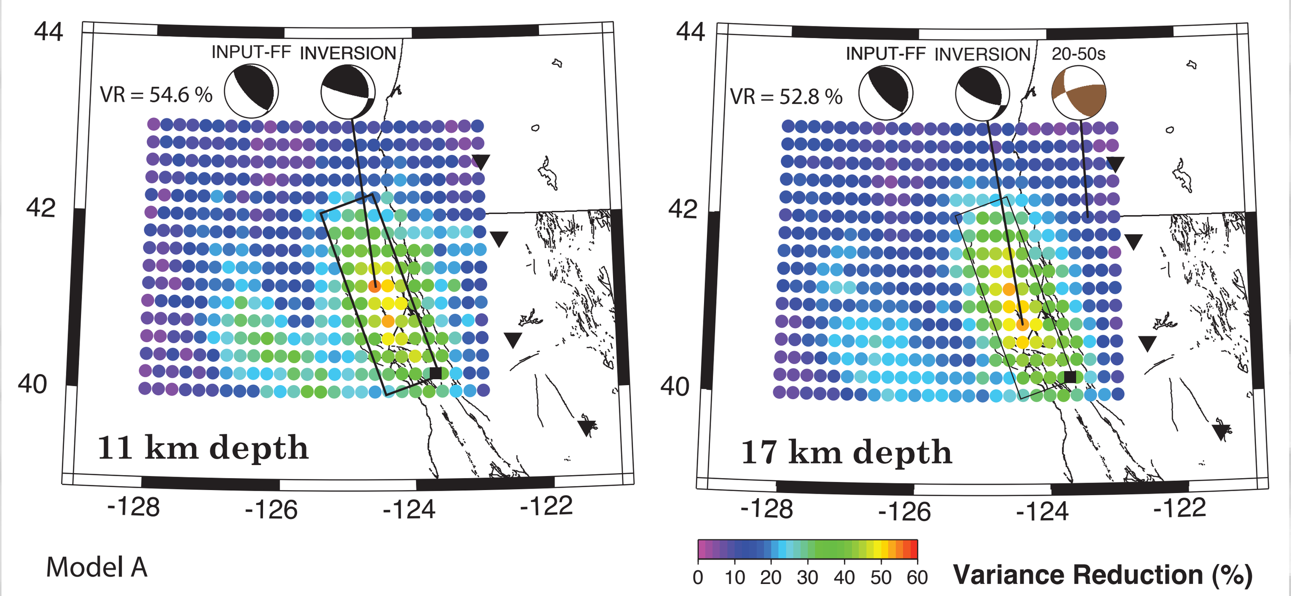

Figure 5: Map of the best VRs obtained at 11 km (left) and 17 km (right) depth for the homogeneous slip rupture.
The rupture segment of the synthetic M8.2 earthquake is shown by the rectangle, the triangles indicate the location of the stations used in the moment tensor analysis. The left mechanism is the input mechanism for the synthetic waveforms and the right one shows our best solution, linked to its location on the grid. The grid points are color-coded by the VR. The brown mechanism is obtained with data filtered between 20 and 50 sec period.

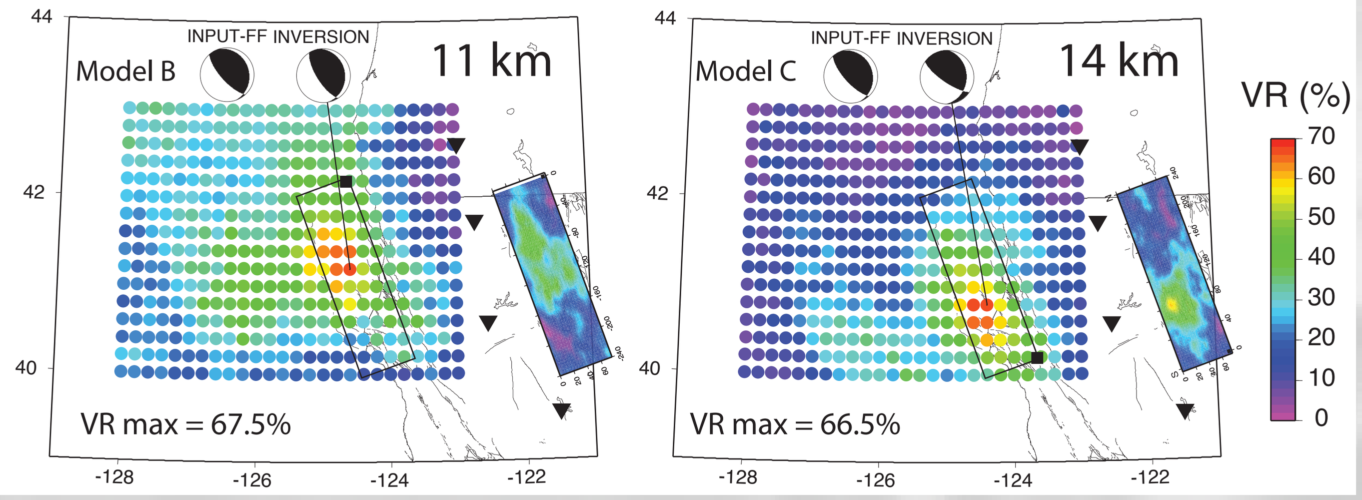

Figure 6: Map of the best VRs obtained at 14 km depth for Model B (left) and Model C (right).
The rupture segment of the synthetic M8.2 earthquake is shown by the rectangle, the triangles indicate the location of the stations used in the moment tensor analysis. The left mechanism is the input mechanism for the synthetic waveforms and the right one shows our best solution, linked to its location on the grid. The grid points are color-coded by the VR. The corresponding slip model is shown on the right of the maps.

We find that the inversions using the 20-50 second passband failed to recover the seismic moment tensor, scalar seismic moment and location for such large earthquakes (Figure 4). The moment magnitude is significantly underestimated yielding only a Mw 6.7, and our best solution shows that the event is located onshore more than 100 km from the centroid of the finite-source model (Figure 5). This is due to the narrow band processing and the Grid MT point-source synthetic is only fitting a small portion of the record, and because of the source corner frequency of the event (1/87sec=0.011 Hz) the inversion is not sensitive to the total moment of the event.

However the 100 to 200 second passband works well and the inversion yields a point-source location near the fault centroid, and a Mw 8.1 with a focal mechanism that recovers a dip-slip mechanism similar to the input mechanism (Figures 5 and 6).

For the heterogeneous models the detections show better VRs than for the homogeneous slip model. This is due to the concentration of slip that is better represented by a point-source assumption. Also it is interesting to notice that the maps of best VRs tend to represent to some degree the slip model of the earthquake.

Multi-point source analysis

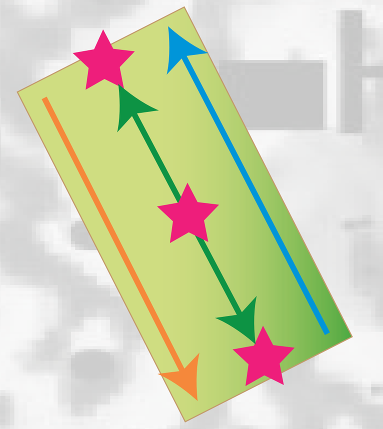

Figure 7: Cartoon of a large thrust earthquake using multi-point source assumption.
The grid points (red stars) on the rupture segment (green rectangle) are summed and considered together without time delay, with a rupture from South to North (blue arrow), from North to South (orange arrow), and bilateral rupture (green arrow).

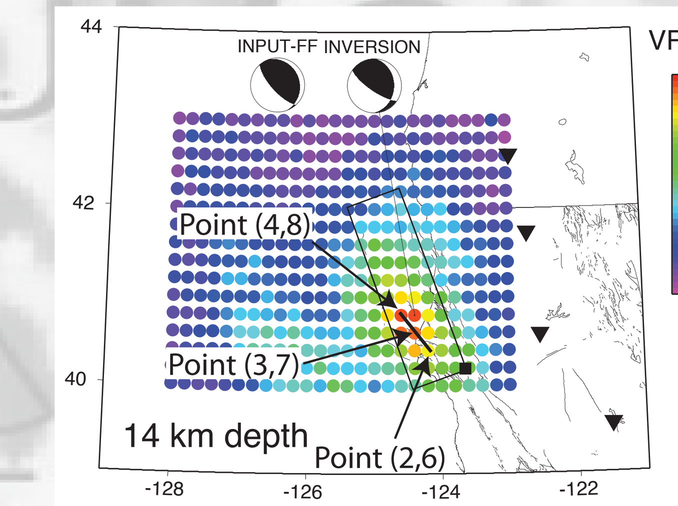

Figure 8: Map showing the points (4,8), (3,7) and (2,6) considered in Figure 9 for the multi-point source analysis (Model C, Figure 6).

In this problem we are considering relatively small distances for the size of the rupture between the stations and the source and the single-point source assumption could fail, especially for a greater thrust earthquake (issue of the near-field).

We are testing the algorithm on multi-point sources, which are obtained after summing single point sources together. Here we present an example using three points of the grid and a rupture from South to North. We show in Figure 9 that a multi-point source assumption can deliver a better source solution of a large magnitude earthquake located within the region.

In addition Figure 10 shows that continuous GPS data if processed in realtime could provide additional constraints on the source of such earthquakes.

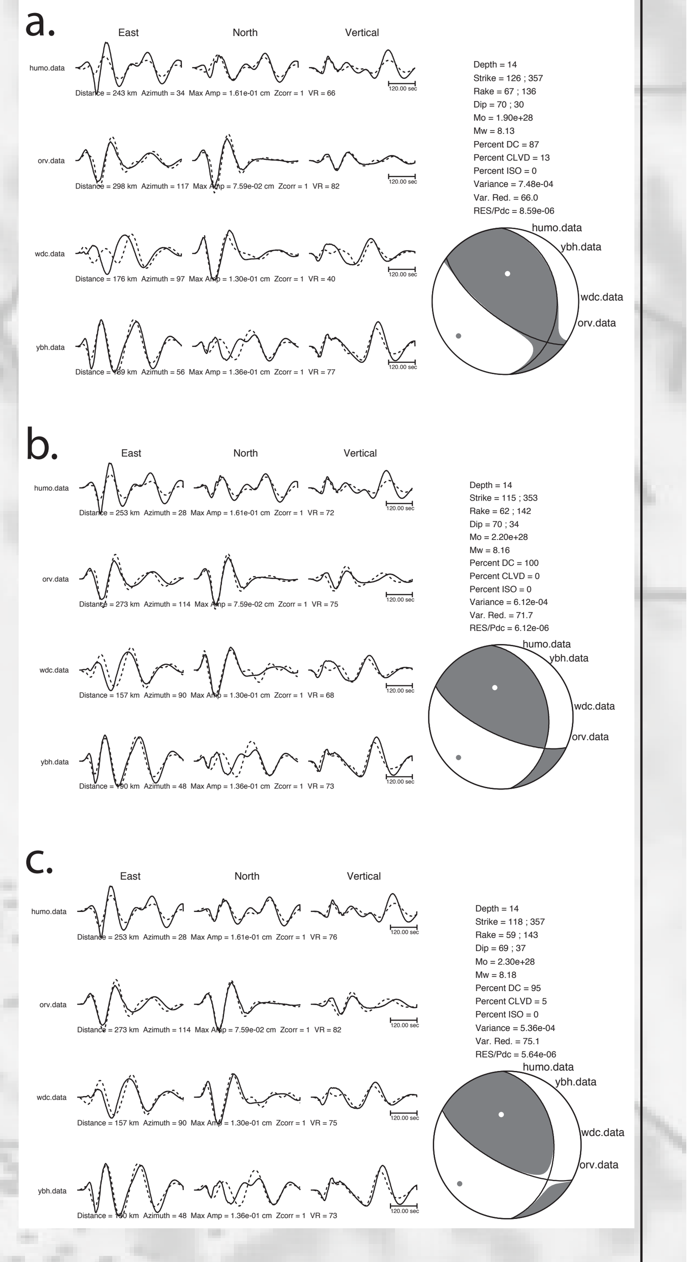

Figure 9: Moment tensor analyses for a M8.2 earthquake (Model C).
a. Best MT analysis obtained considering a single-point source assumption.
b. MT obtained after summing three points (Figure 8). No delay between the sources.
c. MT obtained after summation of the three points and assuming a rupture from South to North and a rupture velocity of 3 km/s. The variance reduction is larger for this solution.

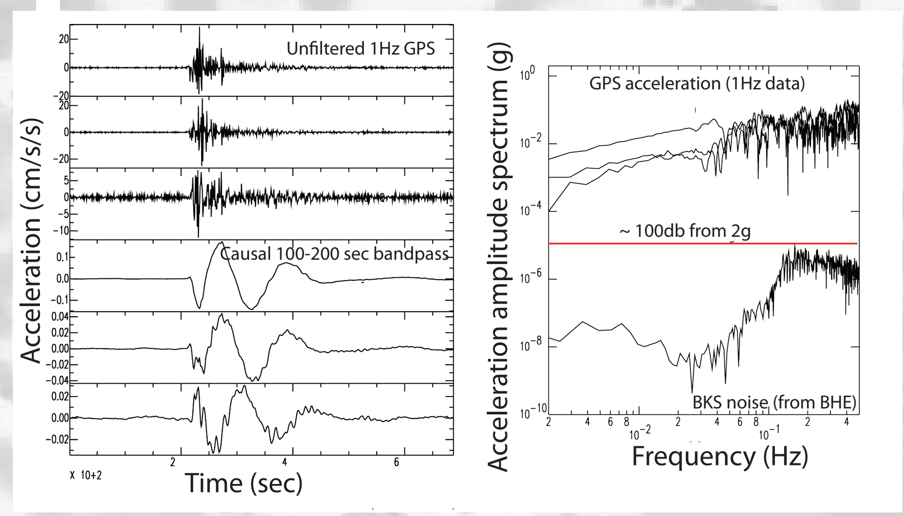

Figure 10: Low frequency accelerations and spectra of the signal from the 1 Hz GPS site located about 111 km SE of the epicenter of the 2010 M8.8 Chile earthquake (from Kristine Larson, Univ. of Colorado).
The similitudes between GPS data and seismic data tend to indicate that the two different datasets could be considered for the detection and source characterization of earthquakes in near-realtime.

Conclusions

Such scanning will provide complete information on the events in realtime using a single stage of processing, and for this reason it will be faster than the current procedures. The method that we are implementing makes use of regional seismic recording stations with continuous realtime telemetry that will enable autonomous detection, location, estimation of scalar seismic moment, and determination of the seismic moment tensor (mode of faulting strike-slip vs. dip-slip faulting) within approximately 8 minutes following the earthquake, before the damaging tsunami waves reach the local coastline. Our efforts for the development of a real-time source parameter reporting system for great earthquakes can be a component of future tsunami early warning system in Northern California.

This project is supported by the U.S. Geological Survey through award G10AP00069 (NEHRP program).

References

Kawakatsu, H., (1998) On the realtime monitoring of the long-period seismic wavefield., Bull. Earth. Res. Inst., 73, 267-274.
Oppenheimer, D., Beroza, G., Carver, G., Dengler, L., Eaton, L., Gee, L., González, F., Jayko, A., Li, W. H., Lisowski, M., Magee, M., Marshall, G., Murray, M., McPherson, R., Romanowicz, B., Satake, K., Simpson, R., Somerville, P., Stein, R. and Valentine, D. (1993), The Cape Mendocino, California, Earthquakes of April 1992: Subduction at the Triple Junction, Science, 261, 433-438.
Tsuruoka, H., H. Kawakatsu, and T. Urabe (2009). GRiD MT (Grid-based Realtime Determination of Moment Tensors) monitoring the long-period seismic wavefield , Phys. Earth Planet. Int., Special issue: Earthquakes in subduction zones: A multidisciplinary approach , vol. 175, pp. 8-16.